
MHD Pulsatile Blood Flow Through an Inclined Stenosed Artery with Body Acceleration and Slip Effects

Emeka Amos¹, Ekakitie Omamoke², Chinedu Nwaigwe¹

¹Department of Mathematics, Rivers State University, Port Harcourt, Nigeria

²Department of Mathematics, Bayelsa Medical University, Yenagoa, Nigeria

Email address:

amos.emeka@ust.edu.ng (E. Amos), ekakitieomamoke@gmail.com (E. Omamoke), omamoke.ekakitie@bmu.edu.ng (E. Omamoke), nwaigwe.chinedu@ust.edu.ng (C. Nwaigwe)

To cite this article:

Emeka Amos, Ekakitie Omamoke, Chinedu Nwaigwe. MHD Pulsatile Blood Flow Through an Inclined Stenosed Artery with Body Acceleration and Slip Effects. *International Journal of Theoretical and Applied Mathematics*. Vol. 8, No. 1, 2022, pp. 1-13.

doi: 10.11648/j.ijtam.20220801.11

Received: January 11, 2022; **Accepted:** January 26, 2022; **Published:** February 9, 2022

Abstract: In this work, the combined effect of slip velocity, pulsatility of the blood flow and body acceleration effect on Newtonian unsteady blood flow past an artery with stenosis and permeable wall is theoretically studied with results discussed. The magnetic field is applied to the stenosed artery with permeable walls which is inclined at a varying angle with the fluid considered to be electrically conducting non-Newtonian elastic-viscous fluid. The momentum equation was transformed from dimensional form to dimensionless form with the Frobenius power series method used to solve the axially symmetric differential momentum equation with suitable boundary conditions. For clarity of the applicability of the study, results was shown graphically with behavior of the blood flow through the artery with stenosis shown for the velocity in the axial direction, blood acceleration, wall shear stress and volumetric flow rate. Results showed that, an increase in the body acceleration G_0 and pulsatile pressure P_1 causes an increase in the blood flow, blood acceleration, shear stress at the artery walls and volumetric flow rate. The increase in the magnetic field M causes a decrease in the blood flow velocity, blood acceleration, shear stress at the artery walls and volumetric flow rate. The increase in the artery inclination ϕ results to an increase in the blood flow velocity, wall shear stress and the volumetric flow rate but an irregular behavior in the blood acceleration while the increase in slip velocity h at the wall decreases the velocity and blood acceleration, while the shear stress at the wall increases and the volumetric flow rate decreases.

Keywords: Magneto-hydrodynamic (MHD), Body Acceleration, Pulsatile Pressure, Slip Velocity, Permeability of the Porous Medium

1. Introduction

The study of blood flow through an artery with stenosis and body acceleration effect is of immense importance in several cardiovascular disease and tumor growth disease. The blood flow that is pulsatile through an artery has gotten a lot of interest from researchers recently due to its relevance in the medical and biomedical sciences. For blood to get to the muscles in the body, it must be pumped from the heart through the arteries in order for blood circulation to be established. Blood circulation occurs such that the heart pumps blood to the various muscles of the body through the arteries. These arteries help to carry the blood to the muscles with the pumping of the blood from the heart in a pulsatile

nature due to the pressure gradient. Hence accumulated deposition of cholesterols, plaques and abnormal tissue growth developed due to thickening of the artery lumen on the walls of the artery will lead to diseases such as stroke gotten from hypertension, hypotension, heart attack and possible tumor and cancer.

Staffman [1] studied the boundary conditions for blood flow at the surface permeable and porous wall with Beaver and Joseph [2] also studying the boundary conditions for blood flow through the permeable walls with the replacement of the slip boundary with slip velocity. McDonald [3], Shukla et al. [4], Srivastava [5] and Misra et al. [6] studied the blood flow through arteries with stenosis at the walls of the artery. Ellahi et al. [7] explained a mathematical model applied for blood

through a catheterized artery that is tapered with composite stenosed artery with further research done by Pralhad *et al.* [8] whose mathematical model for blood flow through an artery with stenosis showing effect of shear stress and resistance at the walls of the artery. Srivastava [9] did an analysis of the blood flow motion that is steady through an artery inclined with applied magnetic field with the conclusion that velocity of the blood flow decreases as a result of the increase in the magnetic field. Haik *et al.* [10] gave a clear distinction between bio-magnetic fluid (BFD) and hydro-magnetic fluid (MHD). The study showed that MHD fluids had electrically conducting properties due to the magnetic field applied to the fluid. Eldesoky [11] did a study on MHD pulsatile unsteady blood flow motion past a porous wall under slip conditions with the results showing that the increase in the height of stenosis and magnetic field causes a decrease in the velocity of the blood flow. Akbardadeh [12] did a study on MHD blood flow past a porous medium with the results from Akbardadeh [12] showing that velocity of the blood flow reduces with increase in porosity of the arterial walls. Gaur and Gupta [13] did a study on unsteady blood flow with slip condition through and artery that is constricted.

Blood flow through the artery is disturbed due to a sudden or quick change in the velocity. A prolonged quick change in the velocity with the body artery inclined at varying angle due to movement of the body during airplane flight, car driving, sudden waking up from sleep, etc., could be very dangerous to the overall wellbeing of the body. Rathod and Tanveer [14] did a study on the pulsatile couple stress fluid flow through a medium that is porous with body acceleration that is periodic and an applied magnetic field to the artery. Saddiqui, *et al.* [15] studied the effect of both the slip velocity and body acceleration on the pulsatile blood flow on a Casson fluid through an artery with stenosis. Sinha *et al.* [16] did a study on the effect of slip on pulsatile blood flow through an artery with stenosed segment with the influence of body acceleration that is periodic. Considering the slip velocity at the wall of the artery the body acceleration which

is periodic, has an influence on the blood flow through an artery with a stenosed segment that is time dependent. Nandal and Kumari [17] studied the slip velocity effect on unsteady peristalsis MHD blood flow past an artery constricted with body acceleration while Bunonyo and Amos [18] studied the effect of the concentration of lipids on the blood flowing through an arterial channel that is inclined with the presence of a magnetic field. An effect of periodic body acceleration and slip velocity on a non-Newtonian blood flow that is unsteady flowing through an artery that is narrow with stenosis and a permeable wall.

In this paper we have done an analysis theoretically, showing the body acceleration, pulsatile pressure, slip velocity and the inclined angle of the body on the non-Newtonian blood flow through an artery with stenosis at the wall. The wall of the artery is considered to be porous and permeable with a detailed analysis done by applying the Frobenius power series method to obtain the solution for the velocity of the blood flow, blood acceleration, wall shear stress and volumetric flow rate with a graphical illustration showing the behavior of the effect of slip velocity, body acceleration, pulsatile pressure gradient, magnetic field and inclined artery on the velocity of the blood flow, blood acceleration, wall shear stress and volumetric flow rate.

2. Formulation of the Problem

The blood flow motion is axisymmetric which passes through an artery with stenosis that is cylindrical and rigid having the coordinates (r', θ', z') lying horizontally in the axis z' with walls which is porous having a permeability that is assumed to have one dimension where the blood is considered to be a non-Newtonian, incompressible viscous electrically conducting fluid influenced by a magnetic field perpendicularly applied to the artery. The stenosis which is formed at the artery depends on the position and height of the constricted wall of the artery.

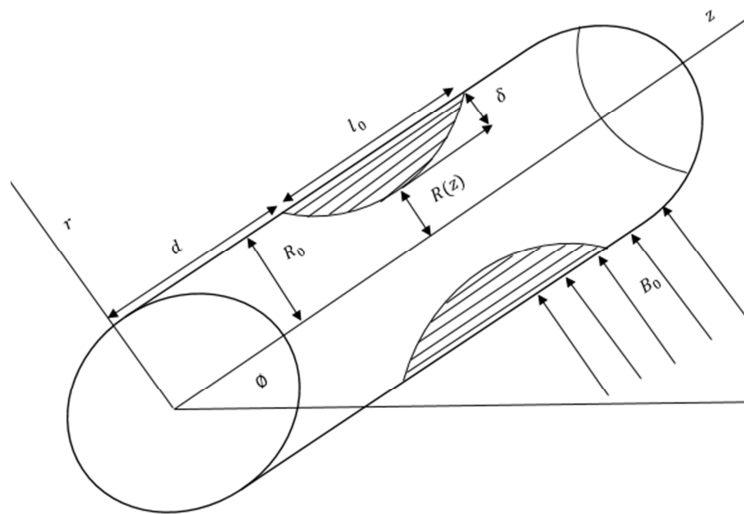


Figure 1. Geometry for stenotic artery.

The flow geometry of the segmented stenotic artery with symmetrical shape in dimensional form proposed by Eldesoky [19] and Kumar et al. [20] is,

$$R(z') = \left\{ \begin{array}{l} d'(z) - \frac{\delta'}{2} \left[1 + \cos \frac{2\pi}{l_0} \left\{ z' - d' - \frac{l'_0}{2} \right\} \right] \\ d'(z) \end{array} \right\}, d' \leq z' \leq d' + l'_0 \quad (1)$$

At the center the maximum height (R) of the stenosis occur, Nadeem et al. [21].

$$z = d + \frac{l_0}{s(s-1)} \text{ For } s \geq 2$$

δ is the height of the stenosis, l_0 is the length of the stenosis, $R(z)$ is the stenotic vessel radius, R_0 is the radius of the normal artery or the non-tapered artery, s is the stenosis shape parameter which determines the shape constriction, $\xi = \tan \phi$ which is the tapering parameter and d is the position of the stenosis.

3. Governing Equation

The blood flow which is pulsatile and flowing past an inclined artery with an applied magnetic field in the radial direction perpendicular to the axial direction is considered:

$$\rho \frac{\partial u'}{\partial t'} = -\frac{\partial p'}{\partial z'} + \rho G(t) + \mu \frac{\partial}{\partial r'} \left(r' \frac{\partial u'}{\partial r'} \right) - \sigma_c B_0^2 u' + g \sin \phi - \frac{\mu}{k_p'} u' \quad (2)$$

The pressure gradient in dimensional form is expressed as

$$-\frac{\partial p'}{\partial z'} = P'_0 + P'_1 \cos(w_p t'); t \geq 0 \quad (3)$$

Where $w_p = 2\pi f_p$ and $w_b = 2\pi f_b$

$$G(t) = G'_0 \cos(w_b t' + \phi); t \geq 0 \quad (4)$$

The boundary condition in dimensional form

$$\left\{ \begin{array}{l} \frac{\partial u'}{\partial r'} = -h' u' \text{ at } r' = R'(z) \\ \frac{\partial u'}{\partial r'} = 0 \text{ at } r' = 0 \end{array} \right\} \quad (5)$$

The dimensionless flow geometry with stenosis, Eldesoky [19] and Kumar et al. [20].

$$R(z) = \left\{ \begin{array}{l} (1 + \xi z) - \frac{\delta}{2} \left[1 + \cos \frac{2\pi}{l_0} \left\{ z - l_1 - \frac{l_0}{2} \right\} \right] \\ (1 + \xi z) \end{array} \right\}, l_1 \leq z \leq l_1 + l_0 \quad (6)$$

The dimensionless Pressure gradient

$$-\frac{\partial p}{\partial z} = P_0 + P_L \cos(w_p t); t \geq 0 \quad (7)$$

The momentum equation in dimensionless form is written as for first consideration:

$$\text{Re} \frac{\partial u}{\partial t} = P_0 + P_L \cos t + G_0 \cos(bt + \phi) + \left(\frac{\partial^2 u}{\partial r^2} + \frac{1}{r} \frac{\partial u}{\partial r} \right) - \left(M^2 + \frac{1}{K} \right) u + \frac{\sin \phi}{\text{Fr}} \quad (8)$$

The dimensional initial and boundary slip conditions are

$$\left\{ \begin{array}{l} \frac{\partial u'}{\partial r'} = -h' u' \text{ at } r' = R'(z) \\ \frac{\partial u'}{\partial r'} = 0 \text{ at } r' = 0 \end{array} \right\} \quad (9)$$

The dimensionless initial and boundary slip conditions are

$$\left\{ \begin{array}{l} \frac{\partial u}{\partial r} = -hu, \text{ at } r = R(z) \\ \frac{\partial u}{\partial r} = 0 \text{ at } r = 0 \end{array} \right\} \quad (10)$$

Where η a constant depending on the porous material properties, K is the permeability parameter.

$$a = \frac{R(z)}{R_0 + \xi z}; h = -\frac{\eta}{R_0 \sqrt{K}}$$

The variable in dimensionless form to transform the governing equations and boundary conditions in dimensionless form.

$$d(z') = R_0 + \xi z'; \delta = \frac{\delta'}{R_0}; u = \frac{u'}{u_0}; l_0 = \frac{l_0'}{R_0}; l_1 = \frac{l_1'}{R_0}; r = \frac{r'}{R_0}; z = \frac{z'}{R_0}; b = \frac{w_b}{w_p}; t = w_p t'; R(z) = \frac{R'(z)}{R_0}; P = \frac{R_0 \rho'}{u_0 \mu}; Re = \frac{\rho \omega R_0'^2}{\mu}; \theta = \frac{T' - T_0}{T'_w - T_0}; C = \frac{C' - C_\infty}{C'_w - C_\infty}; \delta = \frac{\delta'}{R_0}; N^2 = \frac{R_0'^2 Q_0}{\rho c_p k_p}; M^2 = \frac{\sigma R_0'^2 B_0^2}{\mu}; P_e = \frac{\rho R_0'^2 c_p}{k_p}; S_c = \frac{\theta}{D'}; Kr = \frac{E' R_0'^2}{\theta D'}; G_r = \frac{g \rho R_0'^2 \beta_T \theta (T_w - T_0)}{u_0 \mu}; G_C = \frac{g \rho R_0'^2 \beta_C (C_w - C_0)}{u_0 \mu}; P_1 = \frac{P_1' R_0'^2}{u_0 \mu}; P_0 = \frac{P_0' R_0'^2}{u_0 \mu}; G_0 = \frac{\rho G_0' R_0'^2}{u_0 \mu}; f_r = \frac{u_0 \mu}{g R_0'^2}; D = \frac{D'}{D_0}; k = \frac{k_p}{R_0'^2};$$

4. Method of Solution

The modified Bessel function is solved analytically using the Frobenius method. Solutions for the non-linear partial differential governing equation for the steady and pulsatile blood flow velocity expressed as a function of time:

$$u(r, t) = u_0(r) + u_p(r) \varepsilon e^{i\omega t} \quad (11)$$

5. Solution to the Governing Equation

The steady state and pulsatile velocity is expressed below as:

$$\frac{\partial^2 u_0}{\partial r^2} + \frac{1}{r} \frac{\partial u_0}{\partial r} - \beta_1 u_0 = -G \quad (12)$$

$$\frac{\partial^2 u_p}{\partial r^2} + \frac{1}{r} \frac{\partial u_p}{\partial r} - \beta_2 u_p = -F \quad (13)$$

$$\beta_1 = M^2 + \frac{1}{K}; G = P_0 + \frac{\sin \theta}{Fr}; \beta_2 = M^2 + \frac{1}{K} + Rei\omega \text{ and } F = P_1 \cos t + G_0 \cos(bt + \varphi)$$

Using the series solution for the steady state and the pulsatile state which form the Funch's theorem, called the Frobenius series expressed as:

$$\left\{ \begin{array}{l} u_0 = \sum_{n=0}^{\infty} d_n r^{n+k} \text{ Where } d_n, k \in C_1 \\ u_p = \sum_{m=0}^{\infty} d_m r^{m+k} \text{ Where } d_m, k \in C_2 \end{array} \right\} \quad (14)$$

$$u_0 = d_0 r^k \left[1 + \frac{\beta_1 r^2}{(k+2)^2} + \frac{\beta_1^2 r^4}{(k+2)^2(k+4)^2} + \frac{\beta_1^3 r^6}{(k+2)^2(k+4)^2(k+6)^2} + \frac{\beta_1^4 r^8}{(k+2)^2(k+4)^2(k+6)^2(k+8)^2} + \dots \right] \quad (15)$$

The complementary solution for the steady state velocity in the axial direction:

$$u_{0c} = C_1 \left[1 + \frac{\beta_1 r^2}{2^2} + \frac{\beta_1^2 r^4}{2^2 4^2} + \frac{\beta_1^3 r^6}{2^2 4^2 6^2} + \frac{\beta_1^4 r^8}{2^2 4^2 6^2 8^2} + \dots \right] \quad (16)$$

$$\frac{du_{0c}}{dk} = d_0 r^k \ln r \left[1 + \frac{\beta_1 r^2}{(k+2)^2} + \frac{\beta_1^2 r^4}{(k+2)^2(k+4)^2} + \frac{\beta_1^3 r^6}{(k+2)^2(k+4)^2(k+6)^2} + \frac{\beta_1^4 r^8}{(k+2)^2(k+4)^2(k+6)^2(k+8)^2} + \dots \right] + d_0 r^k \left[0 - \frac{2\beta_1 r^2}{(k+2)^3} - \frac{4\beta_1^2 r^4(k+3)}{(k+2)^3(k+4)^3} - \frac{8\beta_1^3 r^6}{(k+2)^3(k+4)^3(k+6)^3} + \frac{16\beta_1^4 r^8}{(k+2)^2(k+4)^2(k+6)^2(k+8)^2} + \dots \right] \quad (17)$$

When $k = 0$,

$$u_{0c} = D_1 \left[\ln r \left(1 + \frac{\beta_1 r^2}{2^2} + \frac{\beta_1^2 r^4}{2^2 4^2} + \frac{\beta_1^3 r^6}{2^2 4^2 6^2} + \frac{\beta_1^4 r^8}{2^2 4^2 6^2 8^2} + \dots \right) + \left(-\frac{\beta_1 r^2}{2^2} - \frac{3\beta_1^2 r^4}{2^3 4^2} - \frac{\beta_1^3 r^6}{4^3 6^3} + \frac{\beta_1^4 r^8}{2^5 6^3 8^3} - \dots \right) \right] \quad (18)$$

$$u_{0c} = C_1 \left[1 + \frac{\beta_1 r^2}{2^2} + \frac{\beta_1^2 r^4}{2^2 4^2} + \frac{\beta_1^3 r^6}{2^2 4^2 6^2} + \frac{\beta_1^4 r^8}{2^2 4^2 6^2 8^2} + \dots \right] + D_1 \left[\ln r \left(1 + \frac{\beta_1 r^2}{2^2} + \frac{\beta_1^2 r^4}{2^2 4^2} + \frac{\beta_1^3 r^6}{2^2 4^2 6^2} + \frac{\beta_1^4 r^8}{2^2 4^2 6^2 8^2} + \dots \right) + \left(-\frac{\beta_1 r^2}{2^2} - \frac{3\beta_1^2 r^4}{2^3 4^2} - \frac{\beta_1^3 r^6}{4^3 6^3} + \frac{\beta_1^4 r^8}{2^5 6^3 8^3} - \dots \right) \right] \quad (19)$$

With $D_1 = 0$, then

$$u_{0c} = C_1 \left[1 + \frac{\beta_1 r^2}{2^2} + \frac{\beta_1^2 r^4}{2^2 4^2} + \frac{\beta_1^3 r^6}{2^2 4^2 6^2} + \frac{\beta_1^4 r^8}{2^2 4^2 6^2 8^2} + \dots \right]$$

The particular solution for the velocity in equation (12)

$$\text{Let } u_{0p} = Q_0; \quad (20)$$

$$u'_{0p} = 0 = u''_{0p} \quad (21)$$

Substitute (20) and (21) into equation (12)

$$\begin{aligned} -\beta_1 Q_0 &= -G \\ Q_0 &= \frac{G}{\beta_1} \end{aligned} \quad (22)$$

The linear combination of (16) and (22) gives the expression for the steady state velocity:

$$u_0(r) = u_{0c}(r) + u_{0p}(r) \quad (23)$$

$$u_0 = C_1 \left[1 + \frac{\beta_1 r^2}{2^2} + \frac{\beta_1^2 r^4}{2^2 4^2} + \frac{\beta_1^3 r^6}{2^2 4^2 6^2} + \frac{\beta_1^4 r^8}{2^2 4^2 6^2 8^2} + \dots \right] + \frac{G}{\beta_1} \quad (24)$$

Applying the boundary condition in equation (9):

$$C_1 \left[\frac{\beta_1 R^2}{2} + \frac{\beta_1^2 R^3}{2^2 4} + \frac{\beta_1^3 R^5}{2^2 4^2 6} + \frac{\beta_1^4 R^7}{2^2 4^2 6^2 8} + \dots \right] = -hC_1 \left[1 + \frac{\beta_1 R^2}{2^2} + \frac{\beta_1^2 R^4}{2^2 4^2} + \frac{\beta_1^3 R^6}{2^2 4^2 6^2} + \frac{\beta_1^4 R^8}{2^2 4^2 6^2 8^2} + \dots \right] - \frac{hG}{\beta_1} \quad (25)$$

$$C_1 = - \frac{\frac{hG}{\beta_1}}{\left[\frac{\beta_1 R^2}{2} + \frac{\beta_1^2 R^3}{2^2 4} + \frac{\beta_1^3 R^5}{2^2 4^2 6} + \frac{\beta_1^4 R^7}{2^2 4^2 6^2 8} + \dots \right] + \left[1 + \frac{\beta_1 R^2}{2^2} + \frac{\beta_1^2 R^4}{2^2 4^2} + \frac{\beta_1^3 R^6}{2^2 4^2 6^2} + \frac{\beta_1^4 R^8}{2^2 4^2 6^2 8^2} + \dots \right]}$$

$$u_p = d_0 r^k \left[1 + \frac{\beta_2 r^2}{(k+2)^2} + \frac{\beta_2^2 r^4}{(k+2)^2 (k+4)^2} + \frac{\beta_2^3 r^6}{(k+2)^2 (k+4)^2 (k+6)^2} + \frac{\beta_2^4 r^8}{(k+2)^2 (k+4)^2 (k+6)^2 (k+8)^2} + \dots \right] \quad (26)$$

When $k = 0$,

$$u_{pc} = d_0 \left[1 + \frac{\beta_2 r^2}{2^2} + \frac{\beta_2^2 r^4}{2^2 4^2} + \frac{\beta_2^3 r^6}{2^2 4^2 6^2} + \frac{\beta_2^4 r^8}{2^2 4^2 6^2 8^2} + \dots \right]$$

$$u_{pc} = C_2 \left[1 + \frac{\beta_2 r^2}{2^2} + \frac{\beta_2^2 r^4}{2^2 4^2} + \frac{\beta_2^3 r^6}{2^2 4^2 6^2} + \frac{\beta_2^4 r^8}{2^2 4^2 6^2 8^2} + \dots \right] \quad (27)$$

$$\begin{aligned} \frac{du_{pc}}{dk} &= d_0 r^k \ln r \left[1 + \frac{\beta_2 r^2}{(k+2)^2} + \frac{\beta_2^2 r^4}{(k+2)^2 (k+4)^2} + \frac{\beta_2^3 r^6}{(k+2)^2 (k+4)^2 (k+6)^2} + \frac{\beta_2^4 r^8}{(k+2)^2 (k+4)^2 (k+6)^2 (k+8)^2} + \dots \right] \\ &+ d_0 r^k \left[0 - \frac{2\beta_2 r^2}{(k+2)^3} - \frac{4\beta_2^2 r^4 (k+3)}{(k+2)^3 (k+4)^3} - \frac{8\beta_2^3 r^6}{(k+2)^3 (k+4)^3 (k+6)^3} + \frac{16\beta_2^4 r^8}{(k+2)^2 (k+4)^2 (k+6)^2 (k+8)^2} + \dots \right] \end{aligned} \quad (28)$$

When $k = 0$,

$$u_{pc} = D_2 \left[\ln r \left(1 + \frac{\beta_2 r^2}{2^2} + \frac{\beta_2^2 r^4}{2^2 4^2} + \frac{\beta_2^3 r^6}{2^2 4^2 6^2} + \frac{\beta_2^4 r^8}{2^2 4^2 6^2 8^2} + \dots \right) + \left(-\frac{\beta_2 r^2}{2^2} - \frac{3\beta_2^2 r^4}{2^3 4^2} - \frac{\beta_2^3 r^6}{4^3 6^3} + \frac{\beta_2^4 r^8}{2^5 6^3 8^3} - \dots \right) \right] \quad (29)$$

$$u_{pc} = C_2 \left[1 + \frac{\beta_2 r^2}{2^2} + \frac{\beta_2^2 r^4}{2^2 4^2} + \frac{\beta_2^3 r^6}{2^2 4^2 6^2} + \frac{\beta_2^4 r^8}{2^2 4^2 6^2 8^2} + \dots \right] + D_2 \left[\ln r \left(1 + \frac{\beta_2 r^2}{2^2} + \frac{\beta_2^2 r^4}{2^2 4^2} + \frac{\beta_2^3 r^6}{2^2 4^2 6^2} + \frac{\beta_2^4 r^8}{2^2 4^2 6^2 8^2} + \dots \right) + \left(-\frac{\beta_2 r^2}{2^2} - \frac{3\beta_2^2 r^4}{2^3 4^2} - \frac{\beta_2^3 r^6}{4^3 6^3} + \frac{\beta_2^4 r^8}{2^5 6^3 8^3} - \dots \right) \right] \quad (30)$$

With $D_2 = 0$, then:

$$u_{pc} = C_2 \left[1 + \frac{\beta_2 r^2}{2^2} + \frac{\beta_2^2 r^4}{2^2 4^2} + \frac{\beta_2^3 r^6}{2^2 4^2 6^2} + \frac{\beta_2^4 r^8}{2^2 4^2 6^2 8^2} + \dots \right]$$

The particular solution for the pulsatile velocity in equation (13):

$$\text{Let } u_{pp} = Q_1 \quad (31)$$

$$u'_{pp} = 0 = u''_{pp} \quad (32)$$

Substitute (31) and (32) into equation (13)

$$\begin{aligned} -\beta_2 Q_1 &= -F \\ Q_1 &= \frac{F}{\beta_2} \end{aligned} \quad (33)$$

The linear combination of (27) and (33) gives the expression for the pulsatile state velocity

$$\begin{aligned} u_p(r) &= u_{pc}(r) + u_{pp}(r) \\ u_p &= C_2 \left[1 + \frac{\beta_2 r^2}{2^2} + \frac{\beta_2^2 r^4}{2^2 4^2} + \frac{\beta_2^3 r^6}{2^2 4^2 6^2} + \frac{\beta_2^4 r^8}{2^2 4^2 6^2 8^2} + \dots \right] + \frac{F}{\beta_2} \end{aligned} \quad (34)$$

Applying the boundary condition in equation (9)

$$C_4 \left[\frac{\beta_2 R^2}{2} + \frac{\beta_2^2 R^3}{2^2 4} + \frac{\beta_2^3 R^5}{2^2 4^2 6} + \frac{\beta_2^4 R^7}{2^2 4^2 6^2 8} + \dots \right] = -h C_4 \left[1 + \frac{\beta_2 R^2}{2^2} + \frac{\beta_2^2 R^4}{2^2 4^2} + \frac{\beta_2^3 R^6}{2^2 4^2 6^2} + \frac{\beta_2^4 R^8}{2^2 4^2 6^2 8^2} + \dots \right] - \frac{hF}{\beta_2} \quad (35)$$

$$C_2 = - \frac{\frac{hF}{\beta_2}}{\left[\frac{\beta_2 R^2}{2} + \frac{\beta_2^2 R^3}{2^2 4} + \frac{\beta_2^3 R^5}{2^2 4^2 6} + \frac{\beta_2^4 R^7}{2^2 4^2 6^2 8} + \dots \right] + \left[1 + \frac{\beta_2 R^2}{2^2} + \frac{\beta_2^2 R^4}{2^2 4^2} + \frac{\beta_2^3 R^6}{2^2 4^2 6^2} + \frac{\beta_2^4 R^8}{2^2 4^2 6^2 8^2} + \dots \right]} \quad (36)$$

Substitute equation (24) and (34) into equation (11) to obtain the solution for the Velocity equation

$$u(r, t) = C_1 \left[1 + \frac{\beta_1 r^2}{2^2} + \frac{\beta_1^2 r^4}{2^2 4^2} + \frac{\beta_1^3 r^6}{2^2 4^2 6^2} + \frac{\beta_1^4 r^8}{2^2 4^2 6^2 8^2} + \dots \right] + \frac{G}{\beta_1} + \left(C_2 \left[1 + \frac{\beta_2 r^2}{2^2} + \frac{\beta_2^2 r^4}{2^2 4^2} + \frac{\beta_2^3 r^6}{2^2 4^2 6^2} + \frac{\beta_2^4 r^8}{2^2 4^2 6^2 8^2} + \dots \right] + \frac{F}{\beta_2} \right) \epsilon e^{i\omega t} \quad (37)$$

The Solution for the Fluid Acceleration equation

$$\begin{aligned} F(r, t) = \frac{du}{dt} &= i\omega \epsilon e^{i\omega t} \left(C_2 \left[1 + \frac{\beta_2 r^2}{2^2} + \frac{\beta_2^2 r^4}{2^2 4^2} + \frac{\beta_2^3 r^6}{2^2 4^2 6^2} + \frac{\beta_2^4 r^8}{2^2 4^2 6^2 8^2} + \dots \right] + \frac{F}{\beta_2} \right) + \epsilon e^{i\omega t} P_l(-\sin t) + i\omega \epsilon e^{i\omega t} P_l(\cos t) + \\ &\epsilon e^{i\omega t} (-b \sin(bt + \varphi)) + G_0(i\omega \cos(bt + \varphi) - b \sin(bt + \varphi)) \end{aligned} \quad (38)$$

The Solution for the Wall Shear Stress equation:

$$\frac{du}{dt} = C_5 \left[\frac{\beta_1 r}{2} + \frac{\beta_1^2 r^3}{2^2 4} + \frac{\beta_1^3 r^5}{2^2 4^2 6} + \frac{\beta_1^4 r^7}{2^2 4^2 6^2 8} + \dots \right] + \left(C_6 \left[\frac{\beta_2 r}{2^2} + \frac{\beta_2^2 r^3}{2^2 4} + \frac{\beta_2^3 r^5}{2^2 4^2 6} + \frac{\beta_2^4 r^7}{2^2 4^2 6^2 8} + \dots \right] \right) \epsilon e^{i\omega t} \quad (39)$$

The Solution for the Volumetric Flow Rate equation:

$$\begin{aligned} Q(r, t) = 2\pi \int_0^a r u(r, t) dr &= 2\pi \left\{ C_5 \left[\frac{a^2}{2} + \frac{\beta_1 a^4}{2^2 4} + \frac{\beta_1^2 a^6}{2^2 4^2 6} + \frac{\beta_1^3 a^8}{2^2 4^2 6^2 8} + \frac{\beta_1^4 a^{10}}{2^2 4^2 6^2 8^2 10} + \dots \right] + \frac{Ga^2}{2\beta_1} + \left(C_6 \left[\frac{a^2}{2} + \frac{\beta_2 a^4}{2^2 4} + \frac{\beta_2^2 a^6}{2^2 4^2 6} + \right. \right. \right. \\ &\left. \left. \frac{\beta_2^3 a^8}{2^2 4^2 6^2 8} + \frac{\beta_2^4 a^{10}}{2^2 4^2 6^2 8^2 10} + \dots \right] + \frac{Fa^2}{2\beta_2} \right) \epsilon e^{i\omega t} \left. \right\} \end{aligned} \quad (40)$$

6. Graphical Results and Discussion

In figure 2, it was seen that the higher the artery inclination ϕ from $15^\circ \leq \phi \leq 60^\circ$, results to an increased blood flow velocity at the artery center but approaches zero at the wall of the stenotic artery. The increase in the blood flow at the wall of the artery results to an increase in both the wall shear stress and the volumetric flow rate in figure 4 and figure 5 but an irregular behavior in the blood acceleration in figure 3.

In figure 6, it was observed that an increase in the body acceleration G_0 causes an increase in the blood flow due to increased work rate of the heart which in return pumps more blood to the muscles. This increase results to an increase in the blood acceleration, shear stress at the artery walls and volumetric flow rate in figure 7 to Figure 9.

In figure 10, it was seen that as the Wormersely number α increased, the velocity of the blood flow decreased. This increase results to a decrease in the blood acceleration, shear stress at the artery walls and volumetric flow rate from figure 11 to Figure 13.

In figure 14, it was seen that as the body acceleration frequency b increased, the velocity of the blood flow decreased. This decrease results to an increase in the blood acceleration in figure 15 but a decrease in the shear stress at the artery walls and volumetric flow rate from figure 16 to Figure 17.

In figure 18, it was seen that an increase in the permeability of the porous wall k causes an increase in the blood flow velocity due to the reduced viscous force at the wall. This increase results to an increase in the blood acceleration, shear stress at the artery walls and volumetric flow rate in figure 19 to Figure 21.

In figure 22, it was seen that an increase in the magnetic field M causes a decrease in the blood flow velocity as a result of increase in the Lorentz force which inhibits blood flow. This decrease results to a decrease in the blood acceleration, shear stress at the artery walls and volumetric flow rate in figure 23 to Figure 25.

As a result of the increase in the work rate of the heart due to body acceleration increase which increases the pulsatile pressure Pl hence resulting to an increase in the blood flow velocity in figure 26. This increase results to an increase in the blood acceleration, shear stress at the artery walls and volumetric flow rate from figure 28 to figure 29.

In figure 30, an increase in Froude's number Fr causes a decrease in the blood flow velocity, shear stress at the artery walls and volumetric flow rate from figure 31 to figure 32. Also, it is seen that the increase in slip velocity h at the wall results to a decrease in the velocity and blood acceleration from figure 33 to figure 34 while the shear stress at the wall increases in figure 35 with a decrease in the volumetric flow rate in figure 36. As the time t increased in figure 37, the velocity of the blood flow decreased but the blood acceleration increased in figure 38 but the wall shear stress and the volumetric flow rate decreased in figure 39 and figure 40.

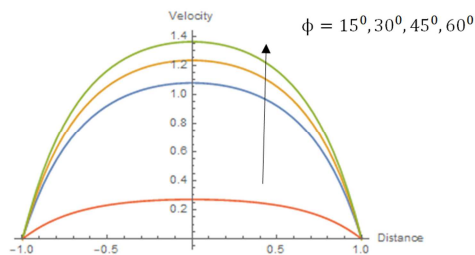


Figure 2. Blood flow velocity distribution for increase in the inclined artery ϕ when $Po = 2, Pl = 4, Go = 3, Fr = 0.05, b = 2, \beta = 30^\circ, k = 0.1, \alpha = 1, h = 1, R = 0.55, M = 1.5, \xi = 0.1, \omega = 1, t = 1$.

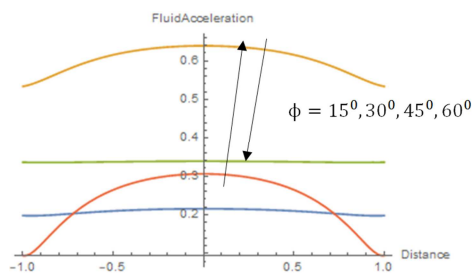


Figure 3. Blood acceleration profile for increase in the inclined artery angle ϕ when $Po = 2, Pl = 4, Go = 3, Fr = 0.05, b = 2, k = 0.1, \alpha = 1, h = 1, R = 0.55, M = 1.5, \xi = 0.1, \omega = 1, t = 1$.

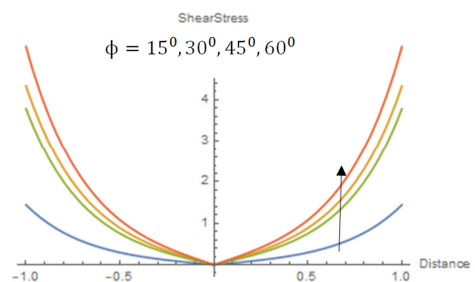


Figure 4. Wall shear stress profile for increase in the inclined artery ϕ when $Po = 2, Pl = 4, Go = 3, Fr = 0.05, b = 2, \beta = 30^\circ, k = 0.1, \alpha = 1, h = 1, R = 0.55, M = 1.5, a = 1, \xi = 0.1, \omega = 1, t = 1$.

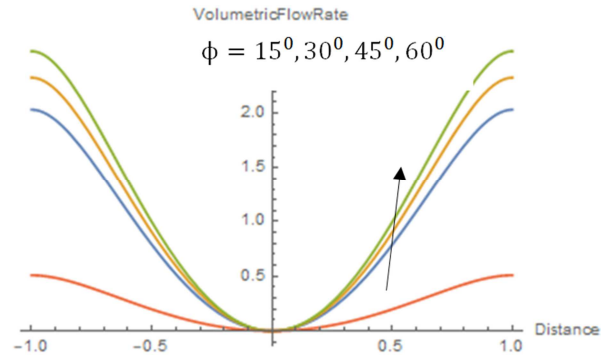


Figure 5. Volumetric flow rate profile for increase in the inclined artery ϕ when $Po = 2, Pl = 4, Go = 3, Fr = 0.05, b = 2, \beta = 30^\circ, k = 0.1, \alpha = 1, h = 1, R = 0.55, M = 1.5, a = 1, \xi = 0.1, \omega = 1, t = 1$.

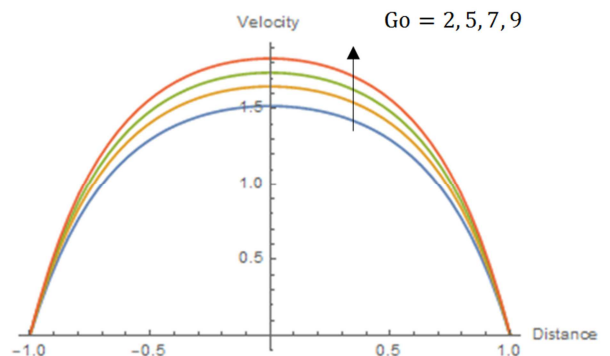


Figure 6. Blood flow velocity distribution for increase in the Body acceleration Go when $Po = 2, Pl = 4, Fr = 0.05, b = 2, \phi = 45^\circ, \beta = 30^\circ, k = 0.1, \alpha = 1, h = 1, R = 0.55, M = 1.5, \xi = 0.1, \omega = 1, t = 1$.

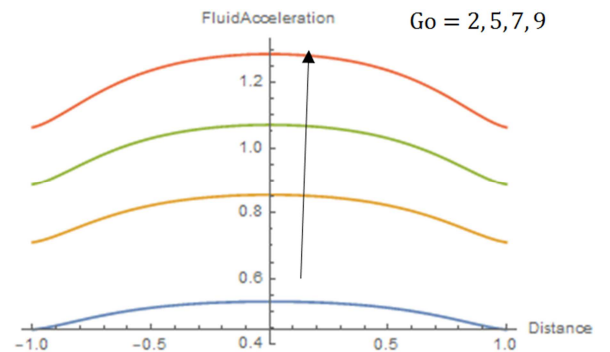


Figure 7. Blood acceleration profile for increase in the Body acceleration Go when $Po = 2, Pl = 4, Fr = 0.05, b = 2, \beta = 30^\circ, k = 0.1, \alpha = 1, h = 1, R = 0.55, M = 1.5, \xi = 0.1, \omega = 1, t = 1$.

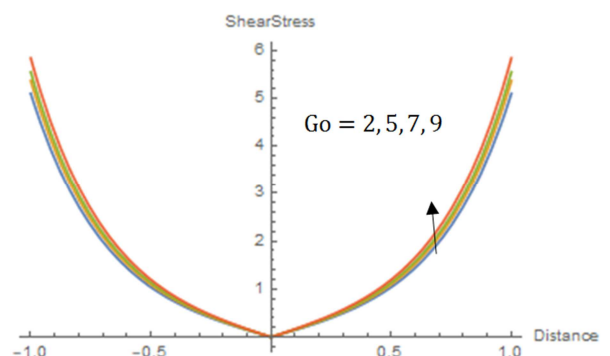


Figure 8. Wall shear stress profile for increase in the Body acceleration Go when $Po = 2, Pl = 4, Fr = 0.05, b = 2, \phi = 45^\circ, \beta = 30^\circ, k = 0.1, \alpha = 1, h = 1, R = 0.55, M = 1.5, a = 1, \xi = 0.1, \omega = 1, t = 1$.

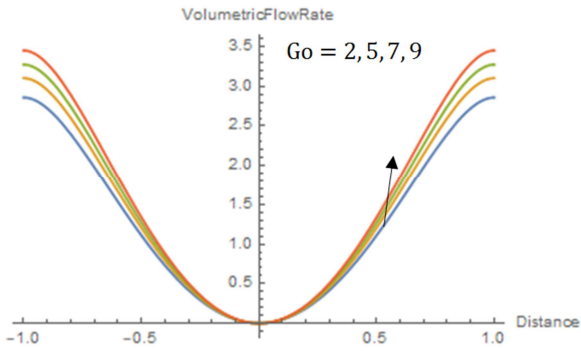


Figure 9. Volumetric flow rate profile for increase in the Body acceleration Go when $Po = 2, Pl = 4, Fr = 0.05, b = 2, \phi = 45^\circ, \beta = 30^\circ, k = 0.1, \alpha = 1, h = 1, R = 0.55, M = 1.5, a = 1, \xi = 0.1, \omega = 1, t = 1$.

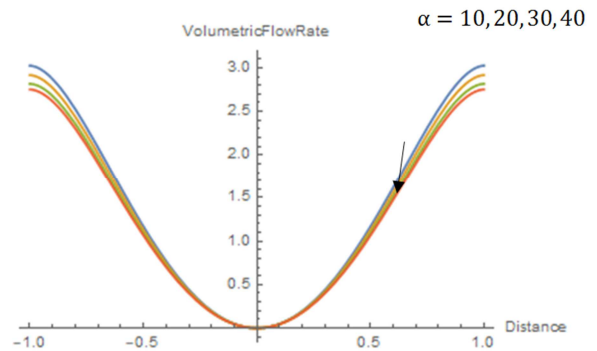


Figure 13. Volumetric flow rate profile for increase in the Womersley Number α when $Po = 2, Pl = 4, Go = 3, Fr = 0.05, b = 2, \phi = 45^\circ, \beta = 30^\circ, k = 0.1, h = 1, R = 0.55, M = 1.5, a = 1, \xi = 0.1, \omega = 1, t = 1$.

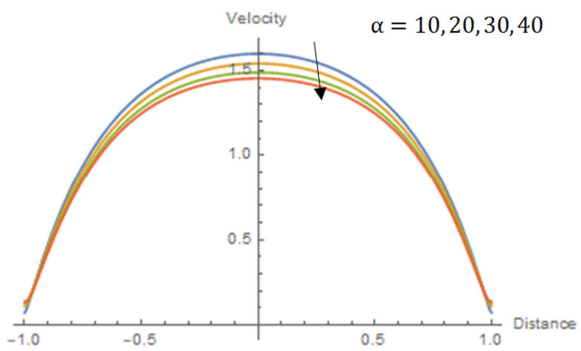


Figure 10. Blood flow velocity distribution for increase in the Womersley Number α when $Po = 2, Pl = 4, Go = 3, Fr = 0.05, b = 2, \phi = 45^\circ, \beta = 30^\circ, k = 0.1, h = 1, R = 0.55, M = 1.5, \xi = 0.1, \omega = 1, t = 1$.

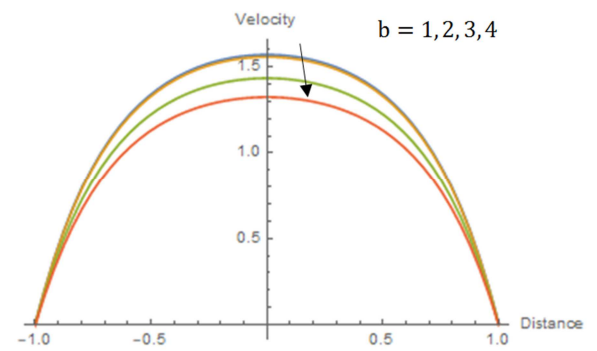


Figure 14. Blood flow velocity distribution for increase in the frequency of body acceleration b when $Po = 2, Pl = 4, Go = 3, Fr = 0.05, \phi = 45^\circ, \beta = 30^\circ, k = 0.1, \alpha = 1, h = 1, R = 0.55, M = 1.5, \xi = 0.1, \omega = 1, t = 1$.

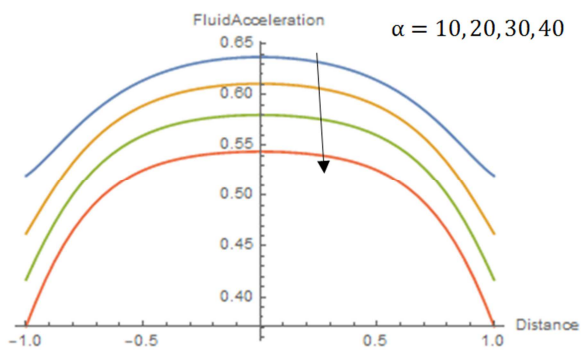


Figure 11. Blood acceleration profile for increase in the Womersley Number α when $Po = 2, Pl = 4, Go = 3, Fr = 0.05, b = 2, \phi = 45^\circ, \beta = 30^\circ, k = 0.1, h = 1, R = 0.55, M = 1.5, \xi = 0.1, \omega = 1, t = 1$.

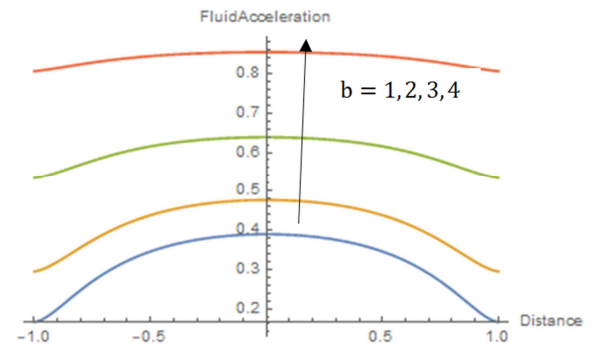


Figure 15. Blood acceleration profile for increase in the frequency of body acceleration b when $Po = 2, Pl = 4, Go = 3, Fr = 0.05, \beta = 30^\circ, k = 0.1, \alpha = 1, h = 1, R = 0.55, M = 1.5, \xi = 0.1, \omega = 1, t = 1$.

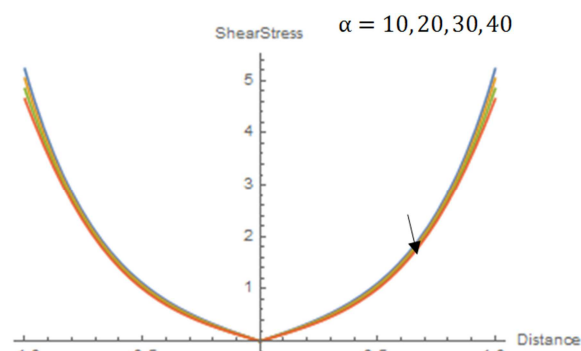


Figure 12. Wall shear stress profile for increase in the Womersley Number α when $Po = 2, Pl = 4, Go = 3, Fr = 0.05, b = 2, \phi = 45^\circ, \beta = 30^\circ, k = 0.1, h = 1, R = 0.55, M = 1.5, a = 1, \xi = 0.1, \omega = 1, t = 1$.

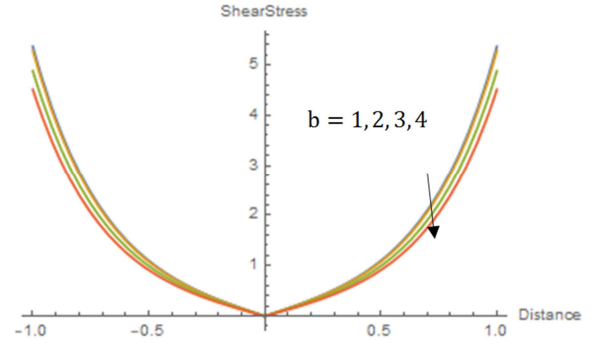


Figure 16. Wall shear stress profile for increase in the frequency of body acceleration b when $Po = 2, Pl = 4, Go = 3, Fr = 0.05, \phi = 45^\circ, \beta = 30^\circ, k = 0.1, \alpha = 1, h = 1, R = 0.55, M = 1.5, a = 1, \xi = 0.1, \omega = 1, t = 1$.

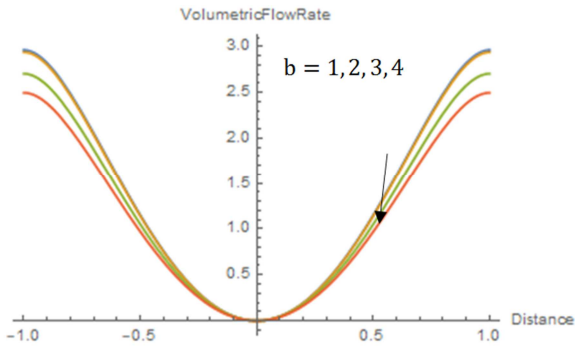


Figure 17. Volumetric flow rate profile for increase in the frequency of body acceleration b when $Po = 2, Pl = 4, Go = 3, Fr = 0.05, \phi = 45^\circ, \beta = 30^\circ, k = 0.1, \alpha = 1, h = 1, R = 0.55, M = 1.5, a = 1, \xi = 0.1, \omega = 1, t = 1$.

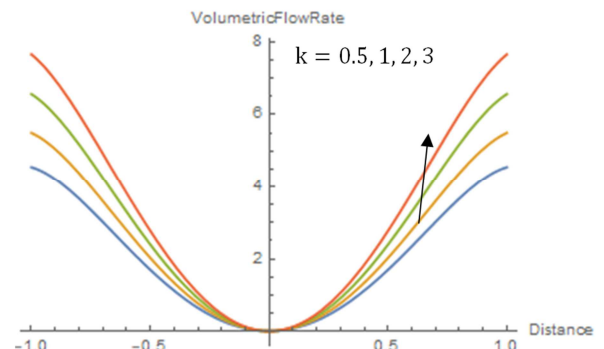


Figure 21. Volumetric flow rate profile for increase in the Permeability of the porous wall k when $Po = 2, Pl = 4, Go = 3, Fr = 0.05, b = 2, \phi = 45^\circ, \beta = 30^\circ, \alpha = 1, h = 1, R = 0.55, M = 1.5, a = 1, \xi = 0.1, \omega = 1, t = 1$.

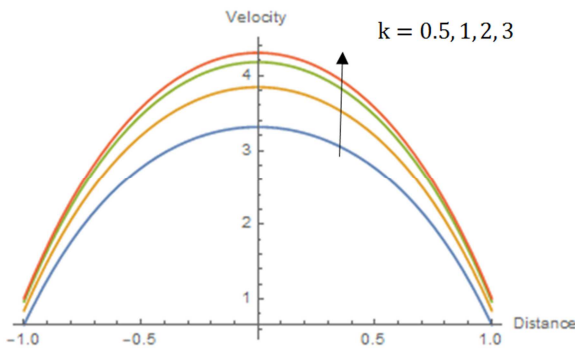


Figure 18. Blood flow velocity distribution for increase in the Permeability of the porous wall k when $Po = 2, Pl = 4, Go = 3, Fr = 0.05, b = 2, \phi = 45^\circ, \beta = 30^\circ, \alpha = 1, h = 1, R = 0.55, M = 1.5, \xi = 0.1, \omega = 1, t = 1$.

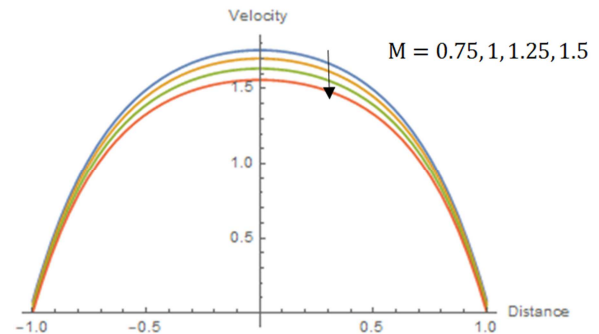


Figure 22. Blood flow velocity distribution for increase in the Magnetic field M when $Po = 2, Pl = 4, Go = 3, Fr = 0.05, b = 2, \phi = 45^\circ, \beta = 30^\circ, k = 0.1, \alpha = 1, h = 1, R = 0.55, \xi = 0.1, \omega = 1, t = 1$.

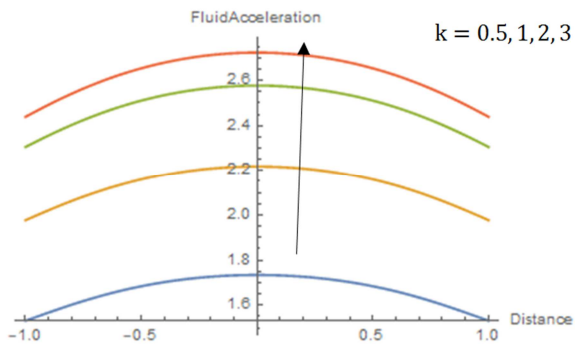


Figure 19. Blood acceleration profile for increase in the Permeability of the porous wall k when $Po = 2, Pl = 4, Go = 3, Fr = 0.05, b = 2, \beta = 30^\circ, \alpha = 1, h = 1, R = 0.55, M = 1.5, \xi = 0.1, \omega = 1, t = 1$.

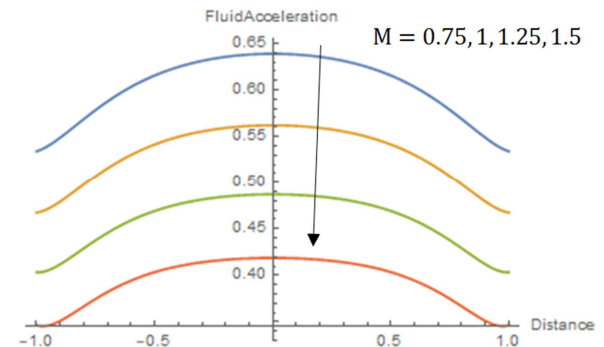


Figure 23. Blood acceleration profile for increase in the Magnetic field M when $Po = 2, Pl = 4, Go = 3, Fr = 0.05, b = 2, \beta = 30^\circ, k = 0.1, \alpha = 1, h = 1, R = 0.55, \xi = 0.1, \omega = 1, t = 1$.

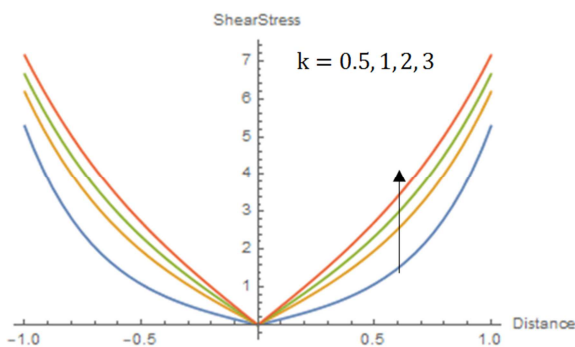


Figure 20. Wall shear stress profile for increase in the Permeability of the porous wall k when $Po = 2, Pl = 4, Go = 3, Fr = 0.05, b = 2, \phi = 45^\circ, \beta = 30^\circ, \alpha = 1, h = 1, R = 0.55, M = 1.5, a = 1, \xi = 0.1, \omega = 1, t = 1$.

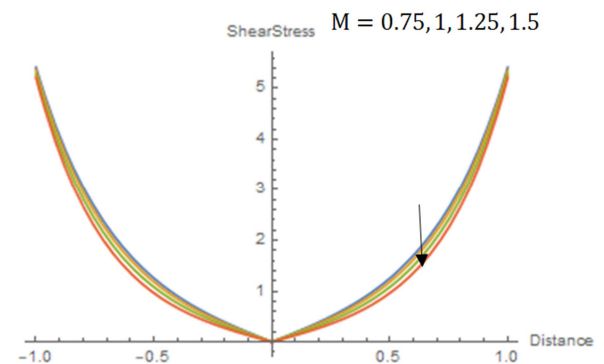


Figure 24. Wall shear stress profile for increase in the Magnetic field M when $Po = 2, Pl = 4, Go = 3, Fr = 0.05, b = 2, \phi = 45^\circ, \beta = 30^\circ, k = 0.1, \alpha = 1, h = 1, R = 0.55, a = 1, \xi = 0.1, \omega = 1, t = 1$.

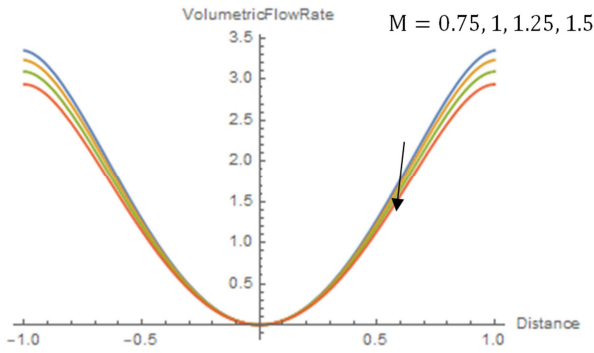


Figure 25. Volumetric flow rate profile for increase in the Magnetic field M when $Po = 2, Pl = 4, Go = 3, Fr = 0.05, b = 2, \phi = 45^\circ, \beta = 30^\circ, k = 0.1, \alpha = 1, h = 1, R = 0.55, a = 1, \xi = 0.1, \omega = 1, t = 1$.

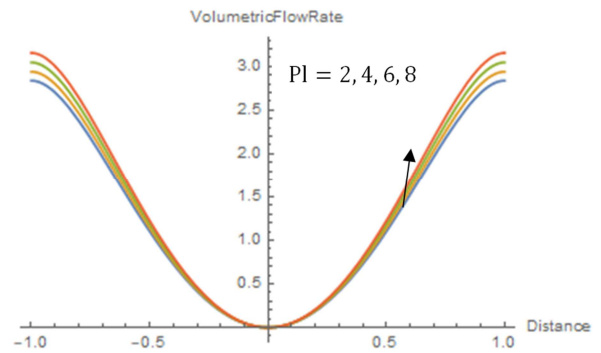


Figure 29. Volumetric flow rate profile for increase in the Pulsatile pressure Pl when $Po = 2, Go = 3, Fr = 0.05, b = 2, \phi = 45^\circ, \beta = 30^\circ, k = 0.1, \alpha = 1, h = 1, R = 0.55, M = 1.5, a = 1, \xi = 0.1, \omega = 1, t = 1$.

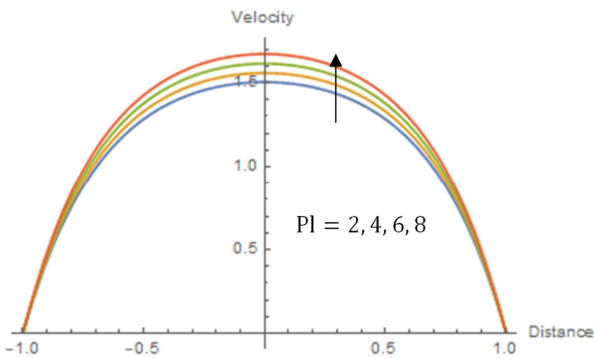


Figure 26. Blood flow velocity distribution for increase in the Pulsatile pressure Pl when $Po = 2, Go = 3, Fr = 0.05, b = 2, \phi = 45^\circ, \beta = 30^\circ, k = 0.1, \alpha = 1, h = 1, R = 0.55, M = 1.5, \xi = 0.1, \omega = 1, t = 1$.

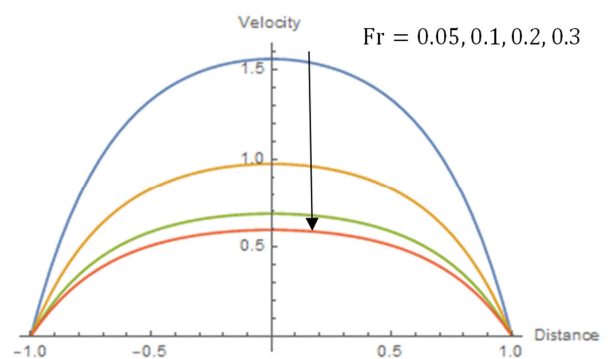


Figure 30. Blood flow velocity distribution for increase in the Froude Number Fr when $Po = 2, Pl = 4, Go = 3, b = 2, \phi = 45^\circ, \beta = 30^\circ, k = 0.1, \alpha = 1, h = 1, R = 0.55, M = 1.5, \xi = 0.1, \omega = 1, t = 1$.

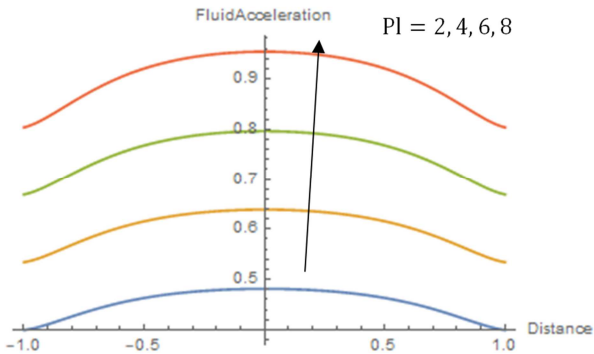


Figure 27. Blood acceleration profile for increase in the Pulsatile pressure Pl when $Po = 2, Go = 3, Fr = 0.05, b = 2, \phi = 45^\circ, \beta = 30^\circ, k = 0.1, \alpha = 1, h = 1, R = 0.55, M = 1.5, \xi = 0.1, \omega = 1, t = 1$.

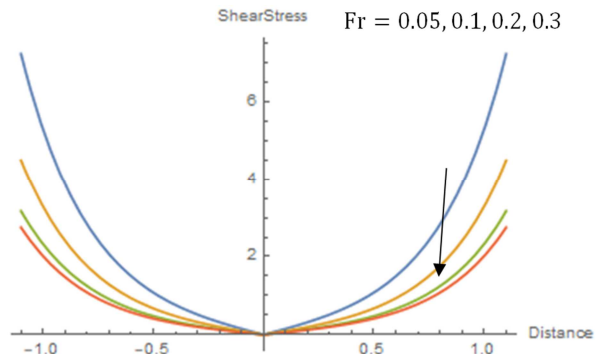


Figure 31. Wall shear stress profile for increase in the Froude Number Fr when $Po = 2, Pl = 4, Go = 3, b = 2, \phi = 45^\circ, \beta = 30^\circ, k = 0.1, \alpha = 1, h = 1, R = 0.55, M = 1.5, a = 1, \xi = 0.1, \omega = 1, t = 1$.

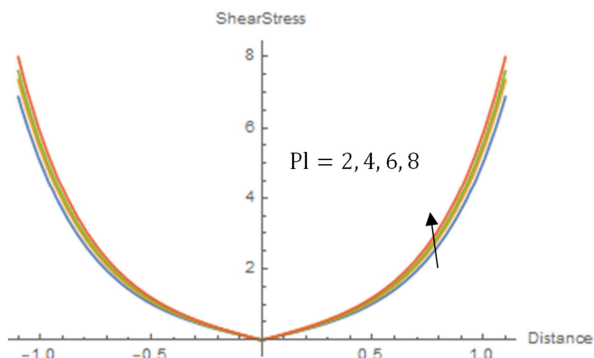


Figure 28. Wall shear stress profile for increase in the Pulsatile pressure Pl when $Po = 2, Go = 3, Fr = 0.05, b = 2, \phi = 45^\circ, \beta = 30^\circ, k = 0.1, \alpha = 1, h = 1, R = 0.55, M = 1.5, a = 1, \xi = 0.1, \omega = 1, t = 1$.

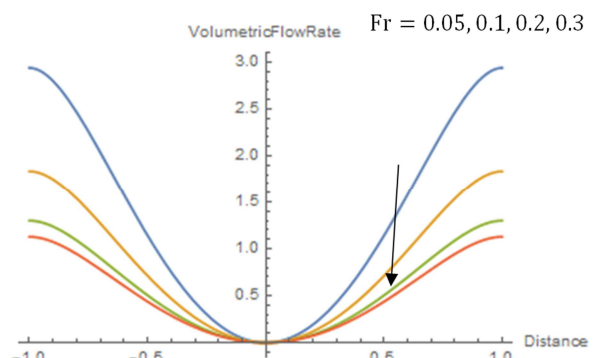


Figure 32. Volumetric flow rate profile for increase in the Froude Number Fr when $Po = 2, Pl = 4, Go = 3, b = 2, \phi = 45^\circ, \beta = 30^\circ, k = 0.1, \alpha = 1, h = 1, R = 0.55, M = 1.5, \xi = 0.1, \omega = 1, t = 1$.

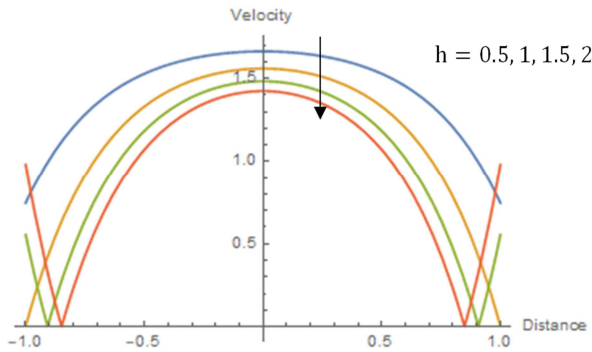


Figure 33. Blood flow velocity distribution for increase in the Slip Parameter h when $Po = 2, Pl = 4, Go = 3, Fr = 0.05, b = 2, \phi = 45^\circ, \beta = 30^\circ, k = 0.1, \alpha = 1, R = 0.55, M = 1.5, \xi = 0.1, \omega = 1, t = 1$.

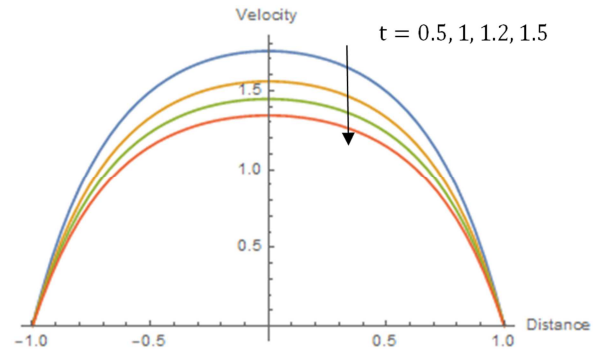


Figure 37. Blood flow velocity distribution for increase in the time t when $Po = 2, Pl = 4, Go = 3, Fr = 0.05, b = 2, \phi = 45^\circ, \beta = 30^\circ, k = 0.1, \alpha = 1, h = 1, R = 0.55, M = 1.5, \xi = 0.1, \omega = 1$.

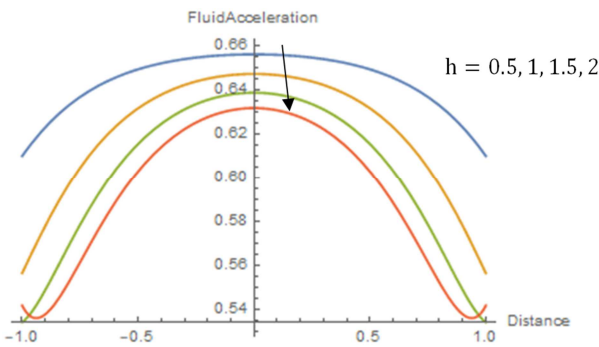


Figure 34. Blood acceleration profile for increase in the Slip Parameter h when $Po = 2, Pl = 4, Go = 3, Fr = 0.05, b = 2, \beta = 30^\circ, k = 0.1, \alpha = 1, R = 0.55, M = 1.5, \xi = 0.1, \omega = 1, t = 1$.

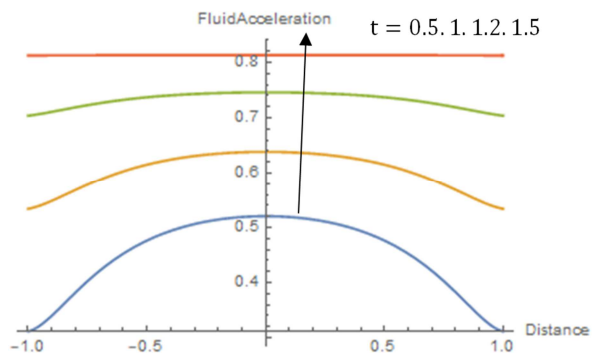


Figure 38. Blood acceleration profile for increase in the time t when $Po = 2, Pl = 4, Go = 3, b = 2, \beta = 30^\circ, k = 0.1, \alpha = 1, h = 1, R = 0.55, M = 1.5, \xi = 0.1, \omega = 1$.

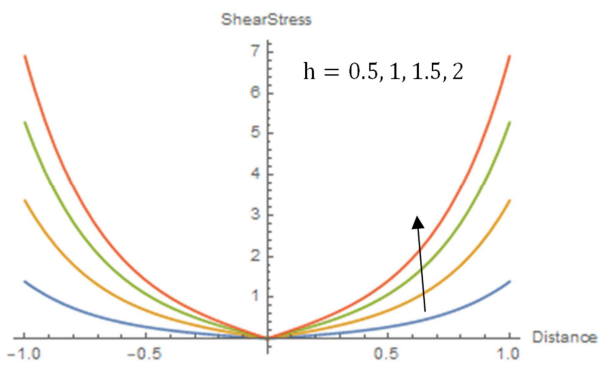


Figure 35. Wall shear stress profile for increase in the Slip Parameter h when $Po = 2, Pl = 4, Go = 3, Fr = 0.05, b = 2, \phi = 45^\circ, \beta = 30^\circ, k = 0.1, \alpha = 1, R = 0.55, M = 1.5, a = 1, \xi = 0.1, \omega = 1, t = 1$.

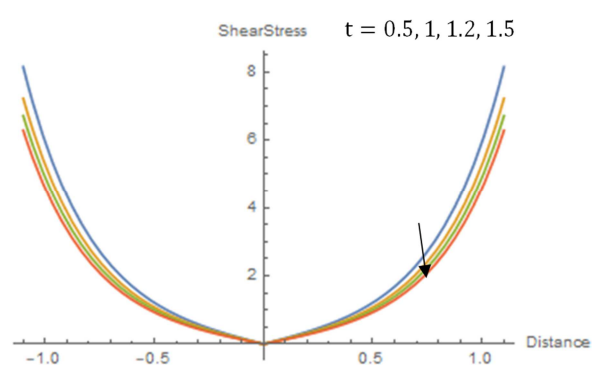


Figure 39. Wall shear stress profile for increase in the time t when $Po = 2, Pl = 4, Go = 3, Fr = 0.05, b = 2, \phi = 45^\circ, \beta = 30^\circ, k = 0.1, \alpha = 1, h = 1, R = 0.55, M = 1.5, a = 1, \xi = 0.1, \omega = 1$.

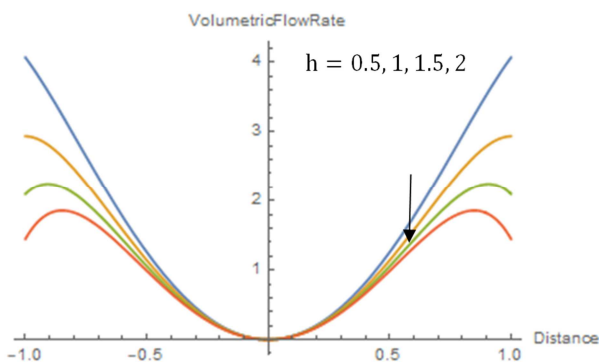


Figure 36. Volumetric flow rate profile for increase in the Slip Parameter h when $Po = 2, Pl = 4, Go = 3, Fr = 0.05, b = 2, \phi = 45^\circ, \beta = 30^\circ, k = 0.1, \alpha = 1, R = 0.55, M = 1.5, a = 1, \xi = 0.1, \omega = 1, t = 1$.

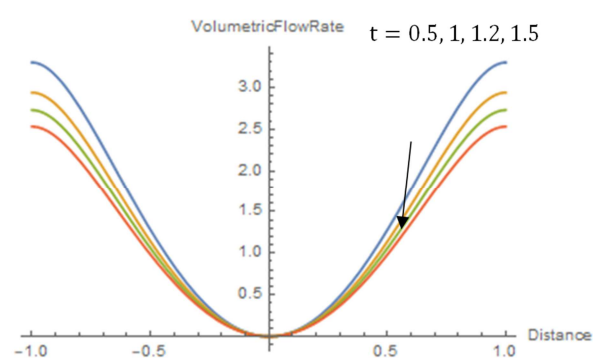


Figure 40. Volumetric flow rate profile for increase in the time t when $Po = 2, Pl = 4, Go = 3, Fr = 0.05, b = 2, \phi = 45^\circ, \beta = 30^\circ, k = 0.1, \alpha = 1, h = 1, R = 0.55, M = 1.5, a = 1, \xi = 0.1, \omega = 1$.

7. Conclusion

This research work has been able to theoretically analyze the combined effect of slip velocity, pulsatility of the blood flow and body acceleration effect on Newtonian unsteady blood flow past an artery with stenosis and permeable wall. The results summarized below showed that, an increase in the body acceleration G_0 causes an increase in the blood flow blood acceleration, shear stress at the artery walls and volumetric flow rate. Hence patients with hypertension are encouraged to reduce their movement through air, land and water or any stress full activity as it could increase their hypertension. On the other hand, patients with hypotension will have an improvement in their health due to increased body acceleration.

The increase in the artery inclination ϕ results to an increase in the blood flow velocity wall shear stress and the volumetric flow rate but an irregular behavior in the blood acceleration.

The increase in the permeability of the porous wall k causes an increase in the blood flow velocity, blood acceleration, shear stress at the artery walls and volumetric flow rate.

The increase in the magnetic field M causes a decrease in the blood flow velocity, blood acceleration, shear stress at the artery walls and volumetric flow rate. This could help improve health conditions among hypertensive patient by putting on a magnetic jacket to help decreased blood flow from the heart to muscles where the heart is overworked.

The increase in the pulsatile pressure P_1 results to the increase in the blood flow velocity, blood acceleration, shear stress at the artery walls and volumetric flow rate. This is a clear proof that the heart is been overworked by pumping more blood to the body muscles due to increased pulsatile pressure. Hence hypertensive patients are encouraged to have more bed rest to improve their health conditions.

Also, it is seen that the increase in slip velocity h at the wall decreases the velocity and blood acceleration, while the shear stress at the wall increases and the volumetric flow rate decreases. This is also a treatment for hypertensive patients due to injection of drugs that induces slip at the section of the stenosed artery. This will help in heart treatment by cleaning the cavities and valves hence treating cardiovascular diseases by controlling blood flow. Studies of the effect of pertinent parameters on MHD fluid flow and MHD blood flow was done by Omamoke and Amos [22] and Omamoke *et al.* [23].

Finally, this research will help medical and health practitioners in administering treatment to hypertensive and hypotensive patients from the predicted outcome in the results of this study.

Nomenclature

P_0 : Steady state pressure gradient
 P_1 : Pulsatile state pressure gradient
 w_p : Frequency of the pulse rate
 w_b : Frequency of the body
 f_p : Frequency of the heart pulse
 f_b : Body acceleration frequency
 G_0 : Body acceleration

$G(t)$: Time dependent body acceleration
 ϕ : Arteries tilted angle
 Φ : Phase difference
 z : Axial blood flow direction
 t : Time
 C : Blood diffusion
 θ : Blood temperature
 g : Acceleration due to gravity
 B_0 : Constant magnetic field
 D : Coefficient of mass Diffusivity
 K : Porosity coefficient
 C_p : Specific heat capacity
 Pe : Peclet number
 Re : Reynolds number
 S_c : Schmidt number
 r : Radial coordinates
 z : Axial coordinate
 ρ : Density of the blood
 μ : Blood viscosity coefficient
 σ_c : Electrical conductivity
 β_T : Coefficient of volume expansion due to temperature
 β_C : Coefficient of volume expansion due to concentration
 σ : Electrical conductivity of the blood
 Kr : Chemical reaction parameter
 N : Radiation parameter
 S_c : Schmidt number
 C_p : Specific heat capacity
 M : Magnetic parameter
 G_r : Grashof temperature number
 β_T : Coefficient of volume expansion due to temperature
 β_C : Coefficient of volume expansion due to concentration.
 G_c : Grashof diffusion number
 θ : Temperature
 C_w : Concentration at the wall,
 T_w : Temperature at the wall
 Q_0 : Heat source parameter.

References

- [1] P., D., Saffman, On the boundary conditions at the surface of a porous medium, *Stud. Appl. Math.*, volume 50, pp. 93-101, (1971).
- [2] G., S. Beaver and D., D. Joseph, Boundary conditions at a naturally permeable wall, *Journal of Fluid Mechanics*, volume 30, pp. 197-207, (1967).
- [3] D., A. McDonald, On steady blood flow through modelled vascular stenosis, *Journal of Biochemistry*, volume 12, pp 13-20, (1979).
- [4] J., B. Shukla, R., S. Parihar and B., R., P. Rao, Effect of stenosis on non-Newtonian flow of blood in an artery, *Bull. Math. Bio.* volume 42, pp. 283 – 294, (1980).
- [5] L., M. Srivastava, Flow of couple stress fluid through stenotic blood vessels, *J. Biomech.*, volume. 1, pp. 479-485, (1985).
- [6] J., C. Misra, M., K. Patra and S., C. Misra, A non-Newtonian model for blood flow through arteries under stenotic conditions, *J. Biomech*, volume 26, pp. 1129-1141, (1993).

- [7] R. Ellahi, S., U. Rahman and S. Nadeem, Blood flow of Jeffery fluid in a catheterized tapered artery with the suspension of Nano particles, *Physics Letter A.*, Volume 378, number 40, pp. 2973-2980.
- [8] R., N. Pralhad and D., H. Schultz, Modelling of arterial stenosis and its modelling to blood disease, *Mathematical Bioscience*, volume 190, number 2, pp. 203-220, (2004).
- [9] N. Srivastava, Analysis of the flow characteristics of blood flowing through an inclined tapered porous artery with mild stenosis under the influence of an inclined magnetic field, *Journal of Biophysics*, (2014).
- [10] Haik Y., Pai V, and Chen C. J. [1999]. Development of magnetic device for cell separation. *Physics of fluids* [1994-present], vol. 17, No. 7, 077103-077118.
- [11] Eldesoky I. M. I. [2014]. Unsteady MHD pulsatile blood flow through porous medium in stenotic channel with slip at permeable walls subjected to time dependent velocity [injection/ suction]. *Walailak journal of science and technology*, vol. 11, No. 11, pp. 901-922.
- [12] Akbarzadeh P. Pulsatile magneto-hydrodynamic blood flows through porous blood vessels using a third grade non-Newtonian fluids model. *Computer methods and programs in biomedicine*, vol. 126, pp. 3-19, (2015).
- [13] M. Gaur, and M., K. Gupta, unsteady slip flow of blood through constricted artery. *Adv. Appl. Sci. Res.*, vol. 6, pp. 49-58, (2015).
- [14] V., P. Rathod and S. Tanveer [2009]; pulsatile flow of couple stress fluid through a porous medium with periodic body acceleration and magnetic field. *Bull. Malaysian Math. Sci.*, vol. 32, pp. 245-259.
- [15] S., U. Saddiqui, S., R. Shah and Geeta, Effect of body acceleration and slip velocity on the pulsatile flow through a casson fluid through stenosed artery, *Adv. Appl. Sci. Res.* Vol. 5, No. 3, pp. 213-225, (2014).
- [16] Sinha, A., Shit, G. C. & Kundu, P. K. (2013). Slip Effect on Pulsatile Flow of Blood through a Stenosed Arterial Segment under Periodic Body Acceleration. *ISRN Biomedical Engineering*, doi.org/10.1155/2013/925876.
- [17] Nandal, J. & Kumari, S. (2019). The effect of slip velocity on unsteady peristalsis MHD blood flow through a constricted artery experiencing body acceleration. *International Journal of Applied Mechanics and Engineering*, Volume 24, No. 3, pp. 645-659.
- [18] Bunonyo, W. K. & Amos, E. (2020). Blood flow through an inclined arterial channel with magnetic field. *Mathematical Modelling and Applications*, 5 (3), 129–137.
- [19] Eldesoky, M. I. (2012). Slip Effects on Unsteady MHD Pulsatile Blood Flow through Porous Medium in an Artery under the Effect of Body Acceleration. *International Journal of Mathematics and Mathematical Sciences*, Volume 2012, ID 860239, doi: 10.1155/2012/860239.
- [20] Kumar, A., Chandel, R. S., Shrivastava, R., Shrivastava, K. & Kumar, S. (2016). Mathematical Modelling of blood flow in an inclined tapered artery under MHD effect through porous medium. *International Journal of Pure and Applied Mathematical Science*, 9 (1), 75–88, ISSN 0972–9828, www.rippublication.com.
- [21] Nadeem, S., Noreen, S. A., Hayat, T. & Awatif, A. H. (2012). Influence of Heat and Mass Transfer on Newtonian Bio magnetic Fluid of Blood Flow through a Tapered Porous Artery with Stenosis. *Transport in Porous Medium*, 91 (1): 81-100.
- [22] Omamoke, E. & Amos, E. (2020). The Impact of Chemical Reaction and Heat source on MHD Free Convection Flow over an Inclined Porous Surface. *International Journal of Scientific and Research Publications*, Volume 10, Issue 5, ISSN 2250-3153, DOI: 10.29322/IJSRP.10.05.2020.p10103.
- [23] Omamoke, E., Amos, E., & Jatari, E. (2020). Impact of Thermal Radiation and Heat Source on MHD Blood Flow with an Inclined Magnetic Field in Treating Tumor and Low Blood Pressure. *Asian Research Journal of Mathematics*, 16 (9), 77-87. <https://doi.org/10.9734/arjom/2020/v16i930221>.